A Temperature-Dependent Nonlinear Analysis of GaN/AlGaN HEMTs Using Volterra Series

Arif Ahmed, *Student Member, IEEE*, Syed S. Islam, *Student Member, IEEE*, and A. F. M. Anwar, *Senior Member, IEEE*

***Abstract*—Gain and intermodulation distortion of an AlGaN/GaN device operating at RF have been analyzed using a general Volterra series representation. The circuit model to represent the GaN FET is obtained from a physics-based analysis. Theoretical current–voltage characteristics are in excellent agreement with the experimental data. For a 1 μm $\times$ 500 μm $Al_{0.15}Ga_{0.85}N$/GaN FET, the calculated output power, power-added efficiency, and gain are 25 dBm, 13%, and 10.1 dB, respectively, at 15-dBm input power, and are in excellent agreement with experimental data. The output referred third-order intercept point (OIP_3) is 39.9 dBm at 350 K and 33 dBm at 650 K. These are in agreement with the simulated results from Cadence, which are 39.34 and 35.7 dBm, respectively. At 3 GHz, third-order intermodulation distortion IM_3 for 10-dBm output power is −72 dB at 300 K and −56 dB at 600 K. At 300 K, IM_3 is −66 dB at 5 GHz and −57 dB at 10 GHz. For the same frequencies, IM_3 increases to −49.3 and −40 dB, respectively, at 600 K.**

***Index Terms*—GaN high electron-mobility transistors, intermodulation distortion, power amplifier, Volterra series.**

I. Introduction

RECENTLY, GaN-based high electron-mobility transistors (HEMTs) are being vigorously pursued for possible applications in microwave circuitry operating at high power and high temperature. A large bandgap (3.4 eV), high breakdown field (3×10^6 V/cm), and high electron mobility (1500 cm^2/V/s) are a few of the attractive properties of GaN-based devices over conventional III–V devices. Recently, Chumbes *et al.* [1] have demonstrated a class-A microwave amplifier with a maximum output power of 4.2 W/mm and a power-added efficiency (PAE) of 36% at 4 GHz for a 1 μm$\times$ 150 μm $Al_{0.35}Ga_{0.65}N$/GaN FET. Power density as high as 9.2 W/mm at 8 GHz from an AlGaN/GaN HEMT on an SiC substrate has also been reported [2]. Using a dual-gate AlGaN/GaN HEMT, Chen *et al.* [3] have demonstrated a PAE of 45%, a gain of 12 dB, and an f_T of 60 GHz. GaN-based FETs have also been successfully demonstrated by Khan *et al.* [4] to operate at elevated temperatures. They have reported f_T and $f_{\max}$ of 22 and 70 GHz, respectively, at 25 °C, which decrease to their corresponding values of 5 and 4 GHz at 300 °C.

The use of GaN-based devices in high-power applications necessitate that a nonlinear analysis of the circuit be carried out. Moreover, the variation of the degree of nonlinearity with temperature is of importance to investigate the device performance at elevated temperatures. In this paper, the effect of nonlinearity in degrading PAE, gain, output power, and the behavior of intermodulation distortion is investigated as a function of temperature. This paper presents a general analysis based on the Volterra series [5], which includes interactions between the nonlinear parameters and spectral components at intermodulation frequencies. Volterra series has been extensively used for the analysis of intermodulation distortion in GaAs MESFETs [6], InGaAs/InAlAs/InP heterojunction bipoloar transistors (HBTs) [7], and AlGaAs/GaAs HBTs [8]. In this paper, the technique is extended to investigate the temperature dependence of nonlinearity and intermodulation distortion of GaN-based HEMTs. The analysis is also implemented on the circuit simulator Cadence so that it may be readily extended to more complex circuits involving multistage amplifiers.

Manuscript received March 30, 2001. The work of A. Ahmed and S. S. Islam was supported by General Electric Industrial Systems under a grant.

The authors are with the Electrical and Computer Engineering Department, University of Connecticut, Storrs, CT 06269-2157 USA.

Publisher Item Identifier S 0018-9480(01)07574-3.

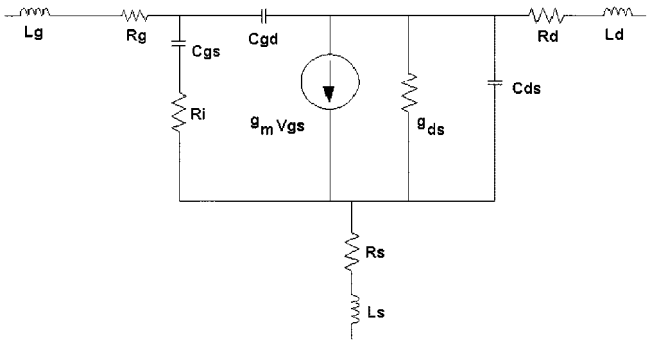

Fig. 1. AlGaN/GaN HEMT equivalent-circuit model.

II. Analysis

The equivalent circuit of the GaN HEMT is shown in Fig. 1. The output resistance $r_{\rm ds}$, transconductance g_m, and the gate–source capacitance $C_{\rm gs}$ are associated with the nonlinearities of the GaN amplifier. The nonlinear circuit parameters $g_m, r_{\rm ds}$, and $C_{\rm gs}$ are represented by a power series expansion up to the third term as [9]

$$g_m = g_{m1} + g_{m2}v_{\rm gs} + g_{m3}v_{\rm gs}^2 \tag{1}$$

$$r_{\rm ds} = r_{\rm ds1} + r_{\rm ds2}v_{\rm gs} + r_{\rm ds3}v_{\rm gs}^2 \tag{2}$$

$$C_{\rm gs} = C_{\rm gs1} + C_{\rm gs2}v_{\rm gs} + C_{\rm gs3}v_{\rm gs}^2. \tag{3}$$

The values of the different terms in the power series for a 1 μm$\times$ 500 μm $Al_{0.15}Ga_{0.85}N$/GaN HEMT are shown in Table I. The determination of the intrinsic circuit parameters proceed by first formulating the charge control based upon a self-consistent solution of Schroedinger and Poisson's equations [10]. The incorporation of the charge control to the

TABLE I
CIRCUIT PARAMETERS FOR A 1 μm× 500 μm $Al_{0.15}Ga_{0.85}N$/GaN HEMT [15] USED IN VOLTERRA-SERIES ANALYSIS

Parameter	T=100 K	T=200K	T=300K	T=400K	T=500K	T=600K
C_{gs1} (pF)	0.5795	0.6226	0.6754	0.7309	0.8191	0.9663
C_{gs2} (pF/V)	-0.1581	-0.1814	-0.2086	-0.2315	-0.28	-0.3668
C_{gs3} (pF/V^2)	0.0567	0.0565	0.0573	0.0567	0.0653	0.0878
g_{m1}(mS/mm)	263.75	221.79	177.33	133.73	89.488	51.64
g_{m2}(mS/mm/V)	275.46	244.63	206.74	163.72	115.68	69.768
g_{m3}(mS/mm/V^2)	-49.085	-32.556	-14.5	2.7313	18.302	24.601
r_{ds1} (kΩ)	395.1	491.992	450.457	588.175	851.343	1000
r_{ds2} (kΩ/V)	-316.772	-398.615	-322.077	-421.463	-616.374	-705.210
r_{ds3} (kΩ/V^2)	84.249	104.863	77.955	100.664	146.691	156.079
C_{gd} (pF)	0.07	0.07	0.07	0.07	0.07	0.07
C_{ds}(pF)	0.05	0.05	0.05	0.05	0.05	0.05
R_d (Ω)	2.5	2.5	2.5	2.5	2.5	2.5
R_i (Ω)	1	1	1	1	1	1
R_s (Ω)	1.7	1.7	1.7	1.7	1.7	1.7

mobility and saturation velocity, as obtained from an ensemble Monte Carlo simulation, eventually provides the theoretical current voltage characteristics, as shown in Fig. 2. The simulation is carried out for a 1 μm× 150 μm $Al_{0.25}Ga_{0.75}N$/GaN HEMT, as reported by Binari *et al.* [11]. As observed, the theoretical results are in excellent agreement with experimental data.

The temperature and bias dependence of the channel electron concentration and the transport parameters make the circuit parameters both temperature and bias dependent. Therefore, circuit nonlinearity is not only bias dependent, but also is a strong function of temperature. The temperature-dependent mobility, as obtained from ensemble Monte Carlo simulation for a 1-μm-long sample, is $\mu_n(T) = -8.7 \times 10^{-5}T^2 - 0.4T + 411$ cm^2/V/s [12]. The above relationship takes into account the effect of nonstationary transport. The saturation velocity decreases from 1.8×10^7 cm/s at 350 K to 1.66×10^7 cm/s at 650 K.

The simplified nonlinear circuit of the GaN-based HEMT amplifier consists of an input signal source $v_s(t)$ with source impedance $Z_s(f)$ and terminated by the load impedance $Z_L(f)$. Using a Volterra series expansion, the output voltage $v_o(t)$ of the nonlinear circuit is expressed as

$$v_o(t) = \int_{-x}^{x} h_1(\tau_1)v_s(t-\tau_1)\,d\tau_1 + \int\int_{-x}^{x} h_2(\tau_1,\tau_2)v_s(t-\tau_1)v_s(t-\tau_2)\,d\tau_1 d\tau_2 + \int\int\int_{-x}^{x} h_3(\tau_1,\tau_2,\tau_3)v_s(t-\tau_1) \times v_s(t-\tau_2)v_s(t-\tau_3)\,d\tau_1\,d\tau_2\,d\tau_3 + \cdots \quad (4)$$

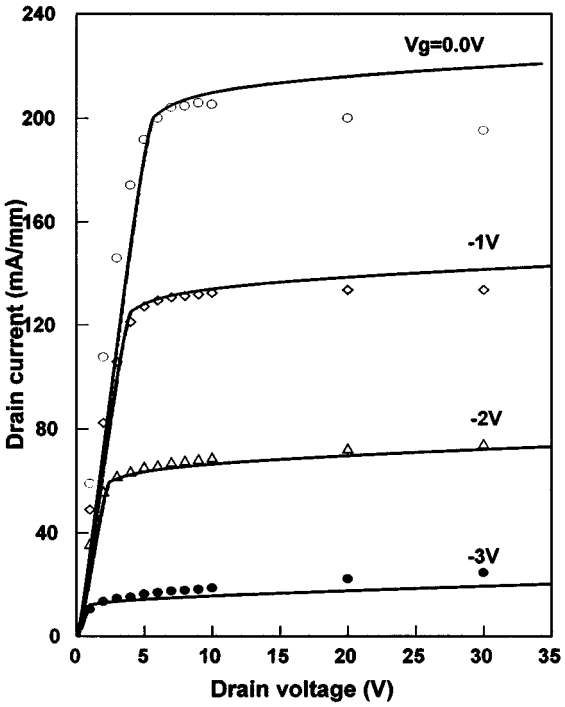

Fig. 2. Calculated (solid line) and experimental (dotted line) current–voltage characteristics for a 1 μm× 150 μm $Al_{0.25}Ga_{0.75}N$/GaN HEMT [11].

where $h_n(\tau_1,\tau_2,\tau_3,\ldots,\tau_n)$ is the nth-order Volterra kernel, whose Fourier transform $H_n(\omega_1,\omega_2,\omega_3,\ldots,\omega_n)$ are the corresponding nth-order nonlinear transfer functions in the frequency domain. Assuming low distortion and mild nonlinearities, the first three terms of the Volterra series are used to characterize the HEMT [5], [9].

The first-order transfer function $H_1(\omega_1)$ expresses the linear response of the amplifier in the frequency domain. The second- and third-order transfer functions $H_2(\omega_1,\omega_2)$ and $H_3(\omega_1,\omega_2,\omega_3)$ are expressed in terms of the circuit parameters to investigate nonlinearity [13], as shown in (5)–(7), at the bottom of this page, where

$$H_{1C}(\omega) = \frac{Y_s(\omega)}{Y_s(\omega)+Y_E(\omega)} \tag{8}$$

$$H_{2C}(\omega_1,\omega_2) = -\frac{\left(\frac{1}{Z_{\rm gs2}}\right)}{Y_i(\omega')}H_{1C}(\omega_1)H_{1C}(\omega_2) \tag{9}$$

$$H_{3C}(\omega_1,\omega_2,\omega_3) = \frac{-1}{Y_i(\omega')}\left[2\left(\frac{1}{Z_{\rm gs2}}\right)H_{1C}(\omega_1)H_{2C}(\omega_1,\omega_2) + \left(\frac{1}{Z_{\rm gs3}}\right)H_{1C}(\omega_1)H_{1C}(\omega_2)H_{1C}(\omega_3)\right] \tag{10}$$

and

$$Y_s(\omega) = \frac{1}{Z_S(\omega)+(R_g+j\omega L_g)} \tag{11}$$

$$Y_E(\omega) = \frac{1}{Z_{\rm gs}(\omega)} \tag{12}$$

$$Y_i(\omega) = Y_s(\omega)+Y_E(\omega) \tag{13}$$

$$Y_o(\omega) = Y_{\rm ds}(\omega)+\frac{1}{(R_d+j\omega L_d)+Z_L(\omega)} \tag{14}$$

$$Y_{\rm ds}(\omega) = g_{\rm ds}(\omega)+j\omega C'_{\rm ds} \tag{15}$$

$$C'_{\rm ds} = C_{\rm ds}+C''_{\rm gd} \tag{16}$$

$$Z_{\rm gs} = \frac{1+j\omega C_{\rm gs}R_i}{j\omega C_{\rm gs}+j\omega C'_{\rm gd}-\omega^2 C_{\rm gs}R_iC'_{\rm gd}} \tag{17}$$

$$Z_{\rm gs2} = \frac{1+j\omega' C_{\rm gs2}R_i}{j\omega' C_{\rm gs2}+j\omega' C'_{\rm gd}-\omega'^2 C_{\rm gs2}R_iC'_{\rm gd}} \tag{18}$$

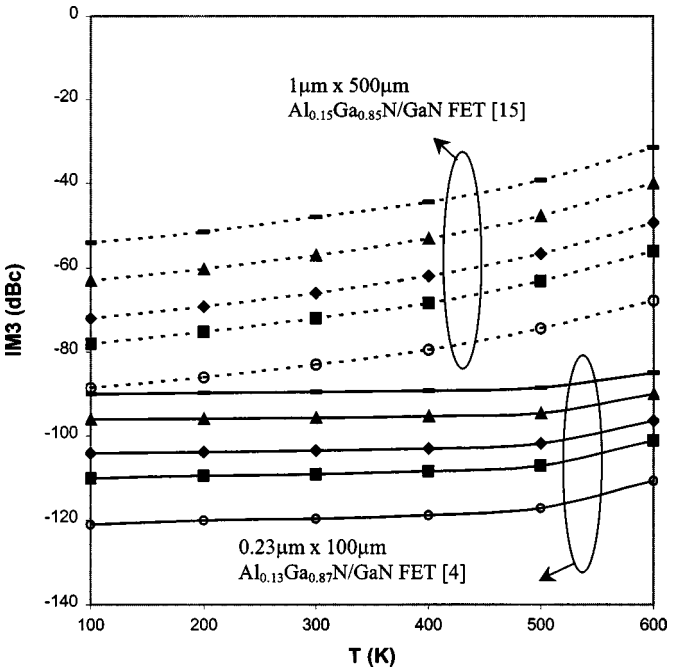

Fig. 3. Third-order intermodulation as a function of temperature for two different gate-length devices [4], [15].

$$Z_{\rm gs3} = \frac{1+j\omega'' C_{\rm gs3}R_i}{j\omega'' C_{\rm gs3}+j\omega'' C'_{\rm gd}-\omega''^2 C_{\rm gs3}R_iC'_{\rm gd}} \tag{19}$$

$$Y_{o2} = (g_{\rm ds2}+j\omega_2 C'_{\rm ds})+\frac{1}{(R_d+j\omega_2 L_d)+Z_L(\omega_2)} \tag{20}$$

$$Y_{03} = (g_{\rm ds3}+j\omega_3 C'_{\rm ds})+\frac{1}{(R_d+j\omega_3 L_d)+Z_L(\omega_3)} \tag{21}$$

$C'_{\rm gd}$ and $C''_{\rm gd}$ are the Miller capacitances replacing $C_{\rm gd}, \omega' = \omega_1+\omega_2$ and $\omega'' = \omega_1+\omega_2+\omega_3$.

$$H_1(\omega) = \frac{-g_m}{Y_o(\omega)}H_{1C}(\omega) \tag{5}$$

$$H_2(\omega_1,\omega_2) = -\frac{H_{1C}(\omega_1)H_{1C}(\omega_2)}{Y_o(\omega')}\left[\frac{-g_{m1}\left(\frac{1}{Z_{\rm gs2}}\right)}{Y_i(\omega')}+g_{m2}+\frac{Y_{\rm ds2}g_{m1}^2}{Y_o(\omega_1)Y_o(\omega_2)}\right] \tag{6}$$

$$H_3(\omega_1,\omega_2,\omega_3) = \frac{-1}{Y_i(\omega')}\left[H_{1C}(\omega_1)H_{1C}(\omega_2)H_{1C}(\omega_3)\left\{g_{m3}-\frac{g_{m1}\left(\frac{1}{Z_{\rm gs3}(\omega'')}\right)}{Y_i(\omega')}-\frac{Y_{o3}g_{m1}^3}{Y_o(\omega_1)Y_o(\omega_2)Y_o(\omega_3)}\right\} + H_{1C}(\omega_1)H_{2C}(\omega_1,\omega_2)\left\{2g_{m2}-\frac{2g_{m1}\frac{1}{Z_{\rm gs2}(\omega'')}}{Y_i(\omega'')}\right\}+2Y_{o2}H_1(\omega_1)H_2(\omega_1,\omega_2)\right] \tag{7}$$

TABLE II
CIRCUIT PARAMETERS FOR A 0.23 μm× 100 μm $Al_{0.13}Ga_{0.87}N$/GaN HEMT [4] USED IN VOLTERRA-SERIES ANALYSIS

Parameter	T=100 K	T=200K	T=300K	T=400K	T=500K	T=600K
C_{gs1} (pF)	0.0371	0.0368	0.0366	0.0364	0.0358	0.0408
C_{gs2} (pF/V)	0.0037	0.0035	0.0032	0.0029	0.0008	-0.0079
C_{gs3} (pF/V^2)	-0.0007	-0.0006	-0.0005	-0.0004	0.0004	0.0028
g_{m1}(mS/mm)	802.63	772.73	732.72	676.85	648.38	461.56
g_{m2}(mS/mm/V)	343.91	341.46	336.11	318.7	357.61	371.32
g_{m3}(mS/mm/V^2)	-79.96	-77.306	-73.046	-67.24	-58.388	10.896
r_{ds1} (kΩ)	156.237	172.982	198.031	228.183	368.609	2000
r_{ds2} (kΩ/V)	-384.114	-442.544	-529.547	-628.207	-1000	-6000
r_{ds3} (kΩ/V^2)	164.129	189.791	228.078	271.292	509.204	2000
C_{gd} (pF)	0.07	0.07	0.07	0.07	0.07	0.07
C_{ds}(pF)	0.05	0.05	0.05	0.05	0.05	0.05
R_d (Ω)	2.5	2.5	2.5	2.5	2.5	2.5
R_i (Ω)	1	1	1	1	1	1
R_s (Ω)	1.7	1.7	1.7	1.7	1.7	1.7

The fundamental and third-order nonlinear output power delivered to the load are expressed in terms of the linear and nonlinear transfer functions as follows [5]:

$$P_{\text{out}_1} = \frac{1}{2}v_{o1}^2 Y_L(\omega_1) = \frac{1}{2}\frac{\text{Re}\left[Z_L(\omega_1)\right]\left|V_s H_1(\omega_1)\right|^2}{\left|Z_L(\omega_1)\right|^2} \tag{22}$$

$$P_{\text{out}_3} = \frac{1}{2}v_{o3}^2 Y_L(2\omega_1-\omega_2) = \frac{1}{2}\frac{\text{Re}\left[Z_L(2\omega_1-\omega_2)\right]\left|V_s^3 H_3(\omega_1,\omega_1,-\omega_2)\right|^2}{\left|Z_L(2\omega_1-\omega_2)\right|^2}. \tag{23}$$

Intermodulation is calculated by applying two equal-amplitude sinusoids of incommensurate frequencies ω_1 and ω_2 to the HEMT input

$$v_s(t) = V_s\cos\omega_1 t + V_s\cos\omega_2 t. \tag{24}$$

The in-band third-order intermodulation products are generated at frequencies $2\omega_1-\omega_2$ and $2\omega_2-\omega_1$. Second- and third-order intermodulation distortions (IM_2 and IM_3) are defined as the ratio of the second- and third-order distorted output power to the fundamental output or desired signal power at ω_1. IM_2 and IM_3 are expressed in terms of the amplifier nonlinear transfer functions as follows [14]:

$$\text{IM}_2 = 20\log_{10}\left[V_s\frac{\left|H_2(\omega_1,\omega_2)\right|}{\left|H_1(\omega_1)\right|}\right] \tag{25}$$

$$\text{IM}_3 = 20\log_{10}\left[\frac{3}{4}V_s^2\frac{\left|H_3(\omega_1,\omega_1,-\omega_2)\right|}{\left|H_1(\omega_1)\right|}\right]. \tag{26}$$

The third-order intercept point, defined as the output power at which the intermodulation-distortion component equals the fundamental frequency output when both are extrapolated linearly from low signal levels, is expressed as [13]

$$\text{IP}_3 = 20\log_{10}\left[\frac{2}{3}\frac{\text{Re}[Z_L]}{|Z_L^2|}\frac{\left|H_1(\omega_1)\right|^3}{\left|H_3(\omega_1,\omega_1,-\omega_2)\right|}\right]. \tag{27}$$

III. RESULTS AND DISCUSSION

In Fig. 3, third-order intermodulation distortion (IM_3) is plotted as a function of temperature. The calculation is carried out for an output power of 10 dBm for varying frequencies. The device simulated is a 1 μm× 500 μm $Al_{0.15}Ga_{0.85}N$/GaN HEMT. The third-order intermodulation distortion increases with temperature, being −72 dB at 300 K and −56 dB at 600 K at 3 GHz. The temperature dependence of IM_3 follows the temperature dependence of transconductance g_m. At 300 K, IM_3 increases with frequency, being −66 dB at 5 GHz and −48 dB at 20 GHz. This is due to the frequency dependence of the nonlinear-circuit elements that causes the higher order distortion powers to increase. IM_3 is dramatically reduced with the reduction of the gate length to 0.23 μm, as shown in Fig. 3, and may be attributed to a higher g_{m1}, as compared to the con-

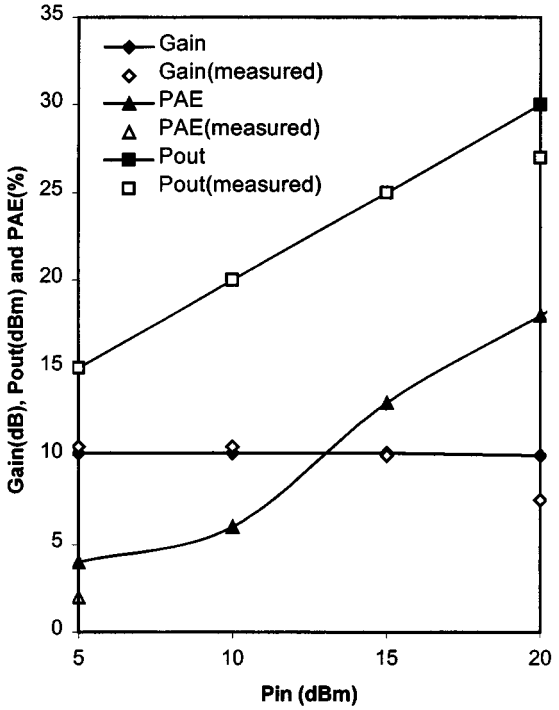

Fig. 4. Gain, PAE, and output power as a function of input power [15].

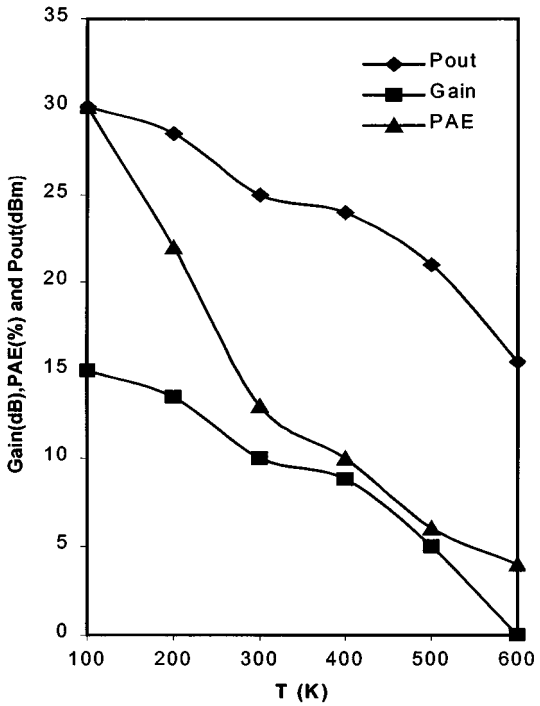

Fig. 5. Gain, PAE, and output power as a function of temperature for 1 μm$\times$ 500 μm $Al_{0.15}Ga_{0.85}N$/GaN FET [15].

tributions from the nonlinear terms (g_{m2} and g_{m3}) with respect to their corresponding values for the 1-μm channel-length device (see Tables I and II).

Fig. 4, shows the calculated gain, PAE, and output power for a 1 μm$\times$ 500 μm $Al_{0.15}Ga_{0.85}N$/GaN FET [15] as a function of input power. At 2 GHz, the calculated PAE of 13%, gain of 10.1 dB, and output power of 25 dBm at 15-dBm input are found to be in excellent agreement with experimental data [15]. Source and load impedance of 50 Ω is considered. The mismatch in the calculated and measured output powers at high input power levels may be attributed to dc and RF power loss present in the circuit. The temperature dependence of the above quantities are investigated for an input power of 15 dBm, as shown in Fig. 5. PAE decreases from 30% to 4%, gain decreases from 15 to 0 dB, and output power decreases from 30 to 15.5 dBm for temperature increasing from 100 to 600 K. With increasing temperature, the decrease in output power, gain, and PAE are correlated to the behavior of the fundamental and third-order transfer functions. The linear transfer function is proportional to the device transconductance that decreases with increasing temperature. However, the third-order transfer function increases with temperature. Therefore, with increasing temperature, the power in the fundamental decreases with a corresponding increase in powers in higher harmonics. For the same operating conditions, a reduction in channel length from 1 μm, for a 1 μm$\times$ 500 μm FET [15], to 0.23 μm, for a 0.23 μm$\times$ 100 μm FET [4], results in a gain that shows a weak temperature dependence, as shown in Fig. 6, and is again attributed to the dominance of g_{m1} over g_{m2} and g_{m3}. The temperature dependence of mobility for the 0.23-μm device, as obtained from ensemble Monte Carlo simulation, is $\mu_n = -1.018 \times 10^{-4}T^2 - 0.1242T + 243$ cm^2/V/s.

In Fig. 7, the frequency-dependent output power and PAE are investigated with an input power of 15 dBm for a source and load

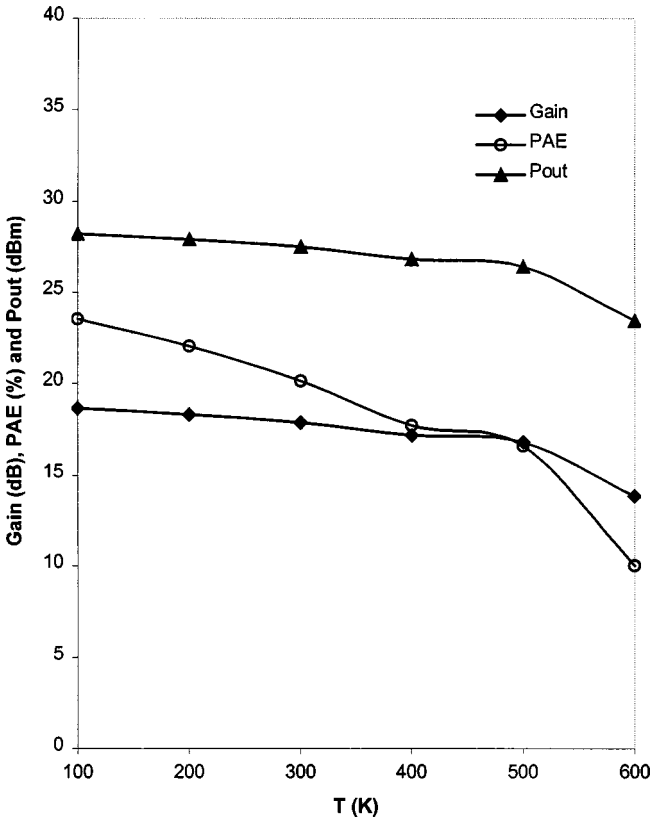

Fig. 6. Gain, PAE, and output power as a function of temperature for 0.23 μm$\times$ 100 μm $Al_{0.13}Ga_{0.87}N$/GaN FET [4].

impedance of 50 Ω. For frequencies increasing from 1 to 10 GHz at 300 K, output power and PAE decrease from 20 to 17.22 dBm and 13.8% to 6.5%, respectively. With increasing frequency, the magnitude of the nonlinear transfer function $H_3(\omega_1, \omega_2, -\omega_2)$

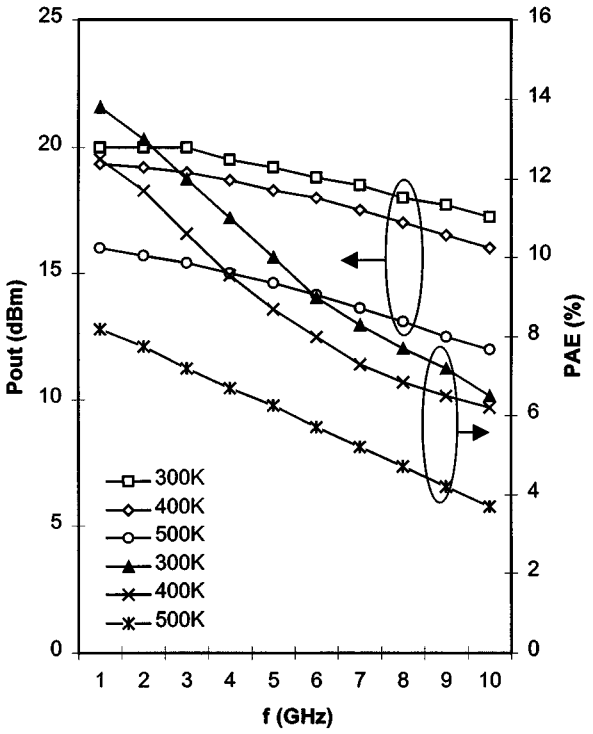

Fig. 7. Output power and PAE as a function of frequency.

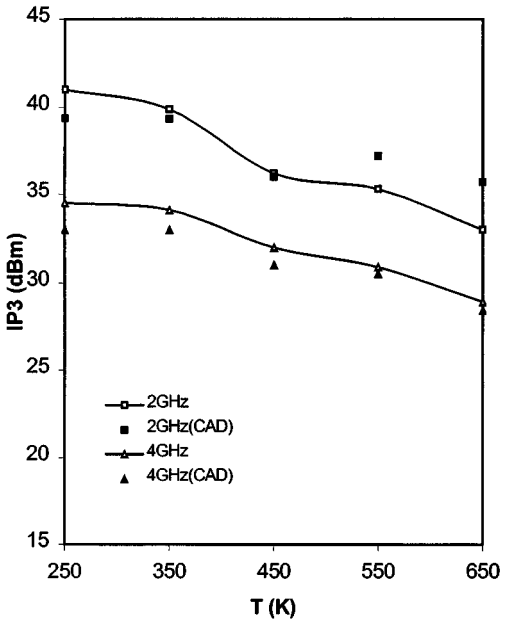

Fig. 8. Output-referred third-order intercept point as a function of temperature.

increases rapidly, resulting in an increment of the third-order distortion power. Within the frequency range considered, the magnitude of $H_1(\omega_1)$ does not change appreciably. As a result, the fundamental output power and PAE decrease with increasing frequency.

Fig. 8 shows the output-referred third-order intercept point as a function of temperature. The amplifier is fed from a 50-Ω signal source and is terminated with a 50-Ω load. The double-tone excitation frequencies are $f_1 = 2$ GHz and 4 GHz with $f_2 = f_1 + \Delta f$ and $\Delta f = 1$ MHz. The theoretical third-order intercept point (IP_3) at 2 GHz is 39.9 dBm at 350 K, which decreases to 33 dBm at 650 K. These numbers are in excellent agreement with the results obtained from Cadence by following the standard procedure. With increasing temperature and frequency, nonlinearity increases, resulting in a lowering of IP_3, as explained within the context of Figs. 5 and 7.

IV. Conclusion

Intermodulation distortion and nonlinearities in a GaN amplifier operating at RF have been analyzed using the general Volterra series. Theoretical calculations for gain, PAE, and P_{out} at room temperature are in agreement with experimental data. With increasing temperature gain, PAE and P_{out} decrease monotonically. Theoretical IP_3 is in excellent agreement with the simulated results obtained from Cadence.

References

[1] E. M. Chumbes, J. A. Smart, T. Prunty, and J. R. Shealy, "Microwave performance of AlGaN/GaN metal insulator semiconductor field effect transistor on sapphire substrate," *IEEE Trans. Electron Devices*, vol. 48, pp. 416–419, Mar. 2001.

[2] J. C. Zolper, "Wide bandgap semiconductor microwave technologies: From promise to practice," in *IEEE IEDM Tech. Dig.*, 1999, pp. 389–392.

[3] C. Chen, R. Coffie, K. Krishnamurthy, S. Keller, M. Rodwell, and U. K. Mishra, "Dual-gate AlGaN/GaN modulation doped field effect transistors with cut off frequencies $f_T > 60$ GHz," *IEEE Electron Device Lett.*, vol. 21, pp. 549–551, Dec. 2000.

[4] M. A. Khan, M. Shur, J. N. Kuznia, Q. Chen, J. Burm, and W. Schaff, "Temperature activated conductance in GaN/AlGaN heterostructure field effect transistors operating at temperature up to 300 °C," *Appl. Phys. Lett.*, vol. 66, no. 9, pp. 1083–1085, Feb. 1995.

[5] S. A. Mass, *Nonlinear Microwave Circuits*. Norwood, MA: Artech House, 1988.

[6] A. M. Crosmun and S. A. Mass, "Minimization of intermodulation distortion in GaAs MESFET small-signal amplifiers," *IEEE Trans. Microwave Theory Tech.*, vol. 37, pp. 1411–1417, Sept. 1989.

[7] B. Li and S. Prasad, "Intermodulation analysis of the collector-up InGaAs/InAlAs/InP HBT using Volterra series," *IEEE Trans. Microwave Theory Tech.*, vol. 46, pp. 1321–1323, Sept. 1998.

[8] J. Lee, W. Kim, Y. Kim, T. Rho, and B. Kim, "Intermodulation mechanism and linearization of AlGaAs/GaAs HBT," *IEEE Trans. Microwave Theory Tech.*, vol. 45, pp. 2065–2072, Dec. 1997.

[9] R. A. Minasian, "Intermodulation distortion analysis of MESFET amplifiers using the Volterra series representation," *IEEE Trans. Microwave Theory Tech.*, vol. MTT-28, pp. 1–8, Jan. 1980.

[10] S. Wu, R. T. Webster, and A. F. M. Anwar, "Physics based intrinsic model for a AlGaN/GaN HEMTs," *MRS Internet J. Nitride Semiconduct.*, vol. 4S1, no. G6.58, 1999.

[11] S. C. Binari, J. M. Redwing, G. Kelner, and W. Kruppa, "AlGaN/GaN HEMT's grown on SiC substrates," *Electron. Lett.*, vol. 33, no. 3, pp. 242–243, Jan. 1997.

[12] A. F. M. Anwar, S. Wu, and R. T. Webster, "Temperature dependent transport properties in GaN, $\mathrm{Al}_x\mathrm{Ga}_{1-x}\mathrm{N}$, and $\mathrm{In}_x\mathrm{Ga}_{1-x}\mathrm{N}$ semiconductors," *IEEE Trans. Electron Devices*, vol. 48, pp. 567–572, Mar. 2001.

[13] J. J. Bussgang, L. Ehrman, and J. W. Graham, "Analysis of nonlinear systems with multiple inputs," *Proc. IEEE*, vol. 62, pp. 1088–1119, Aug. 1974.

[14] B. Razavi, *RF Microelectronics*. Englewood Cliffs, NJ: Prentice-Hall, 1998.

[15] Y.-F. Wu, S. Keller, P. Kozodoy, B. P. Keller, P. Parikh, D. Kapolnek, P. Denbaars, and U. K. Mishra, "High power AlGaN/GaN HEMT's for microwave applications," *Solid State Electron.*, vol. 41, no. 10, pp. 1569–1574, Oct. 1997.

Arif Ahmed (S'96) was born in Tangail, Bangladesh. He received the B.S. degree in electrical engineering from the Regional Institute of Technology, Jamshedpur, India, in 1996, and is currently working toward the M.S. degree in electrical and computer engineering at the University of Connecticut, Storrs.

He is currently with the Electrical and Computer Engineering Department. University of Connecticut, Storrs. His research concerns the analysis and design of GaN-based devices and circuits operating at RF.

Syed S. Islam (S'00) received the B.S. degree in electrical and electronic engineering from the Bangladesh University of Engineering and Technology (BUET), Dhaka, Bangladesh, in 1993, the M.S. degree in electrical engineering from the University of Saskatchewan, Saskatoon, SK, Canada, in 2000, and is currently working toward the Ph.D. degree in electrical engineering at the University of Connecticut, Storrs.

From 1994 to 1997, he was a faculty member in the Department of Electrical and Electronic Engineering, BUET. From 1997 to 1999, he was a Research Assistant in the Department of Electrical Engineering, University of Saskatchewan. Since 2000, he has been a Research/Teaching Assistant in the Department of Electrical and Computer Engineering, University of Connecticut. His research interests include the modeling and simulation of microwave and millimeter-wave semiconductor devices and circuits, numerical techniques, and the design, modeling, and simulation of microwave amplifiers.

Mr. Islam is a member of the IEEE Microwave Theory and Techniques Society (IEEE MTT-S).

A. F. M. Anwar (S'86-M'88-SM'00) received the B.S. and M.S. degrees in electrical and electronic engineering from the Bangladesh University of Engineering and Technology (BUET), Dhaka, Bangladesh, in 1982 and 1984, respectively, and the Ph.D. degree from Clarkson University, Potsdam, NY, in 1988.

He is currently a Professor in the Department of Electrical and Computer Engineering, University of Connecticut, Storrs, where his research group in the RF Microelectronics and Noise Laboratory is currently involved in the study of transport in short heterostructures and antimony-based HEMTs operating above 300 GHz. Moreover, his group is involved in modeling GaN-based high-power HEMTs and HBTs. He is also active in research in the areas of CMOS-based class-E amplifiers, as well as transport dynamics and noise in resonant tunneling diodes (RTDs) and one-dimensional (1-D) structures.

Dr. Anwar is an editor for the IEEE TRANSACTIONS ON ELECTRON DEVICES.